International Journal of Mechanical, Industrial and Aerospace Sciences
ISSN: 2517-9950
Vol:1, No:12, 2007

Aeroelastic Response for Pure Plunging Motion of a Typical Section Due to Sharp Edged Gust, Using Jones Approximation Aerodynamics

M. H. Kargarnovin and A. Mamandi

***Abstract*—**This paper presents investigation effects of a sharp edged gust on aeroelastic behavior and time-domain response of a typical section model using Jones approximate aerodynamics for pure plunging motion. Flutter analysis has been done by using *p* and *p-k* methods developed for presented finite-state aerodynamic model for a typical section model (airfoil). Introduction of gust analysis as a linear set of ordinary differential equations in a simplified procedure has been carried out by using transformation into an eigenvalue problem.

***Keywords*—**Aeroelastic response, Jones approximation, Pure plunging motion, Sharp edged gust.

I. Introduction [1]

In a more complete unsteady aerodynamic theory, the lift and pitching moment consist of two parts from two physically different phenomena namely: noncirculatory and circulatory effects. Noncirculatory effects, also called apparent mass and inertia effects, are generated when the wing motion has nonzero acceleration. It has to then carry with it a part of the air surrounding it. That air has finite mass, which leads to inertial forces opposing its acceleration

Circulatory effects are generally more important for aircraft wings. Indeed, in steady flight it is the circulatory lift that keeps the aircraft aloft. Vortices are an integral part of the process of generation of circulatory lift. Basically, there is a difference in the velocities on the upper and lower surfaces of an airfoil. Such a velocity profile can be represented as a constant velocity flow plus a vortex. In a dynamic situation, the strength of the vortex (i.e., the circulation) is changing with time. However, the circulatory forces of steady-flow theories do not include the effects of the vortices shed into the wake.

Restricting our discussion to two dimensions and potential flow, we recall an implication of the Helmholtz theorem i.e. the total vorticity will always vanish within any closed curve surrounding a particular set of fluid particles. Thus, if some clockwise vortices develop about the airfoil, a counterclockwise vortex of the same strength has to shed into the flow. As one of generated wake moves along this shed vortex then it changes the flow field by inducing an unsteady flow back onto the airfoil. This behavior is a function of the strength of shed vortex and its distance away from the airfoil. Thus, the effect of shed vorticity is in general a very complex undertaking and would necessitate knowledge of each and every vortex shed in the flow. However, if one assumes that the vortices shed in the flow move with the flow, then one can estimate the effect of these vortices [1].

There are two types of unsteady aerodynamic theories, both of which are based on potential flow theory and take into account the effects of shed vorticity. The simpler theory is appropriate for classical flutter analysis as well as for the *k* and *p-k* methods. The other is a finite-state theory cast in time domain, appropriate for time-domain analysis as well as for eigen-analysis in the form of the *p* method [1-4].

Peters et al. [5] presented a new finite state aerodynamic theory for incompressible, two–dimensional flow around thin airfoils by directly governing equations derived from potential flow theory with no assumptions on the time history of airfoil motions. Ghadiri and Razi [6] studied the limit cycle oscillations of rectangular cantilever wings containing cubic nonlinearity in an incompressible flow. A numerical methodology coupling Navier–Stokes equations and structural modal equations for predicting 3-D transonic wing flutter has been developed by Chen et al. [7]. Moosavi, et al. [8] proposed a procedure developed based on Galerkin method to predict the speed and frequency in which flutter occurs by using finite element structural for the wing with three DOF cantilever beam. Stochastic behavior of panels in supersonic flow has been investigated to assess the significance of including the damping caused by the strains resulting from axial extension of the panel in the paper presented by Fazelzadeh et al. [9]. Svacek et al. [10] developed a numerical simulation of flow induced airfoil vibrations with large amplitudes. Haddadpour et al. [11] evalutated of quasi-steady aerodynamic modeling for flutter prediction of an aircraft wing in incompressible flow. Also Qin, Marzocca and

Manuscript received Oct 25, 2007.

Mohammad H. Kargarnovin, Professor, Aerospace Engineering Department, Faculty of Mechanical Engineering, Science and Research Branch, Islamic Azad University, Tehran, Iran and Mechanical Engineering Department, Sharif University of Technology, Tehran, Iran, e-mail: mhkargar@sharif.edu

Ahmad Mamandi, Ph.D. student, Aerospace Engineering Department, Faculty of Mechanical Engineering, Science and Research Branch, Islamic Azad University, Tehran, Iran; e-mail: am_2001h@ yahoo.com.

Librescu [12] studied the aeroelastic instability and response of advanced aircraft wings at subsonic flight speeds.
The review of above literatures revealed that the Theodorsen's unsteady thin-airfoil theory and Jones approximate model can be used to analysis the airfoil vibrations under different free air stream velocity with respect to flutter speed.

II. Theodorsen's Unsteady Thin-Airfoil Theory and Jones Approximation

Theodersen in 1934 derived a theory of unsteady aerodynamics for a thin airfoil undergoing small oscillations in incompressible flow. The lift contains both circulatory and noncirculatory terms, whereas the pitching moment about the quarter-chord is entirely noncirculatory. According to the Theodorsen's theory, the lift (L) and pitching moment (M) are [1]:

$$L = 2\pi\rho_\infty UbC(k)\left[\dot{h}+U\theta+b(\frac{1}{2}-a)\dot{\theta}\right]+\pi\rho_\infty b^2(\ddot{h}+U\dot{\theta}-ba\ddot{\theta}) \quad (1)$$

$$M_{\frac{1}{4}} = -\pi\rho_\infty b^3\left[\frac{1}{2}\ddot{h}+U\dot{\theta}+b\left(\frac{1}{8}-\frac{a}{2}\right)\ddot{\theta}\right] \quad (2)$$

Moreover the generalized forces Q_h and Q_θ are given as [1]:

$$\begin{cases} Q_h = -L, \\ Q_\theta = M_{\frac{1}{4}} + b(\frac{1}{2}+a)L \end{cases} \quad (3)$$

The function $C(k)$ is a complex-valued function of the reduced frequency k, given by [1]

$$C(k) = \frac{H_1^{(2)}(k)}{H_1^{(2)}(k)+iH_0^{(2)}(k)} \quad (4)$$

Where $H_n^{(2)}(k)$ are Hankel function of the second kind which can be expressed in terms of Bessel functions of the first and second kind, respectively, as [1]

$$H_n^{(2)}(k) = J_n(k) - iY_n(k) \quad (5)$$

The function $C(k)$ is called Theodorsen's function and its variation is plotted in Fig. 1. Note that $C(k)$ is real and equal to unity for the steady case (i.e., for $k=0$). As k increases, one finds that the imaginary part increases in magnitude while the real part decreases. As k tends to infinity, $C(k)$ approaches to ½. However, for practical situations k does not exceed values of the order of unity. Hence, the plot in Fig. 1 only extends to $k=1$. When any harmonic function is multiplied by $C(k)$, its magnitude is reduced and a phase lag is introduced.[1]
A few things are noteworthy concerning Eqs. (1-2). First, in Theodorsen's theory lift-curve slope is equal to 2π. Thus, the first of two terms in the lift is the circulatory lift without the effect of shed vortices multiplied by $C(k)$. The multiplication by $C(k)$ is a consequence of the theory having taken into account the effect of shed vorticity. The second term in the lift as well as the pitching moment is noncirculatory, depending on the acceleration and angular acceleration of the airfoil. The circulatory lift is the more significant of the two terms in the lift.

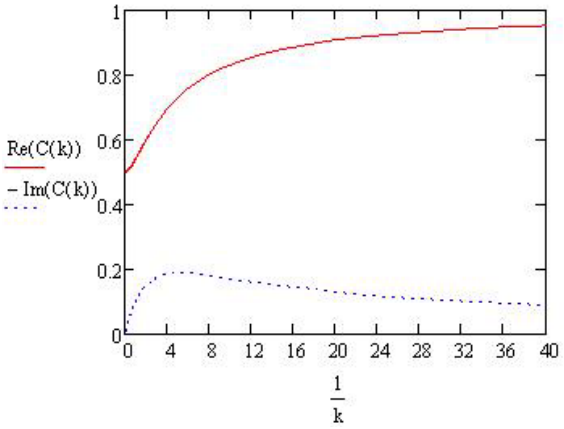

Fig. 1 real part and imaginary part of Theodorsen's function

At this paper by considering the Jones approximation aerodynamics model and based on the strip theory and 2D incompressible unsteady aerodynamics [1-4], under assumptions of zero sweep angle and positive plunging deflection in the upward motion in Z direction, the unsteady aerodynamic lift and aerodynamic twist moment are obtained for the first time about the elastic axis. Under this assumption, the total lift and moment expressions including the circulatory forces become [1] and [5]:

$$L = -\pi\rho_\infty b^2\left[\ddot{w}-U\dot{\theta}+ba\ddot{\theta}\right] - C_{L_\alpha}\rho_\infty Ub\left[\frac{1}{2}\left(\dot{w}-U\theta+ba\dot{\theta}-\frac{b}{2}(\frac{C_{L_\alpha}}{\pi}-1)\dot{\theta}\right)+\sum_{i=1}^{n}\gamma_i B_i\right] \quad (6)$$

and

$$M_{ea} = -\pi\rho_\infty b^3\left[\frac{1}{2}\left(\frac{C_{L_\alpha}}{\pi}-1\right)U\dot{\theta}-Ua\dot{\theta}+a\ddot{w}+\left(\frac{1}{8}+a^2\right)b\ddot{\theta}\right] - C_{L_\alpha}\rho_\infty Ub^2\left(\frac{1}{2}+a\right)\left[\frac{1}{2}(\dot{w}-U\theta+ba\dot{\theta}-\frac{b}{2}\left(\frac{C_{L_\alpha}}{\pi}-1\right)\dot{\theta} + \sum_{i=1}^{n}\gamma_i B_i\right] \quad (7)$$

where $b=2C$ in which C is the chord length, ρ_∞ is the free stream air density, U is the free air stream velocity and a is elastic axis to mid chord distance. In addition, "." and ".." above any parameter, indicate the first and second derivative with respect to the time, respectively. Moreover,

$C_{L_\alpha} = 2\pi$ for airfoils and B_i satisfies

$$\dot{B}_i + \left(\beta_i \frac{U}{b}\right) B_i = w_{0.75C} \tag{8}$$

in which $w_{0.75C}$ is equal to [1]:

$$w_{0.75C} = \dot{w} - U\theta + ba\dot{\theta} - \frac{b}{2}\left(\frac{C_{L_\alpha}}{\pi} - 1\right)\dot{\theta} \tag{9}$$

and

$$\gamma_i = \frac{U}{b}\beta_i \alpha_i \tag{10}$$

The constants α_i, β_i are some constant coefficients used in the quasi-polynomial approximation of the Wagner function $\Phi_w(\tau)$ [1-3]:

$$\Phi_w(\tau) = 1 - \sum_{i=1}^{n} \alpha_i \exp(-\beta_i \tau) H(\tau) \tag{11}$$

and are given in Table (1)

Table (1): The coefficients used in the approximation of the Wagner function [2]

α_1	α_2	β_1	β_2
0.165	0.335	0.0455	0.300

At this stage for the case of pure oscillatory plunging motion using the above aerodynamics we should find the nondimensional lift as followings.

First we assume an imaginary exponential form for B and w such as: $B = \bar{B} e^{j\omega t}$ and $w = \bar{w} e^{j\omega t}$ in which $j = \sqrt{-1}$ and $\omega = \frac{kU}{b}$.

By substituting Eq. (9) into Eq.(8) we have

$$(j\omega)\bar{B} e^{j\omega t} + \beta \frac{U}{b} \bar{B} e^{j\omega t} = -(j\omega)\bar{w} e^{j\omega t} \tag{12}$$

By some further simplifications one would get:

$$\bar{w} = \left(\frac{j\omega + \beta_i \frac{U}{b}}{-j\omega}\right)\bar{B} = (-1 + \frac{j}{k}\beta_i)\bar{B} \tag{13}$$

For only a pure plunging motion the lift force reduces to:

$$L = -\pi\rho_\infty(-\ddot{w}) - C_{L_\alpha}\rho_\infty U b(-\dot{w} + \sum_{i=1}^{n}\gamma_i B_i) \tag{14}$$

From Eq. (13) we get:

$$\bar{B} = \frac{1}{-1 + \frac{j}{k}\beta_i}\bar{w} \tag{15}$$

or

$$\bar{B} = -\frac{k(k + j\beta_i)}{k^2 + \beta_i^2}\bar{w} \tag{16}$$

where in our case taking *i=1* and *2* will lead us to an acceptable accuracy in our obtained results.

By substituting Eq. (16) into the Jones unsteady aerodynamics, one would get:

$$L = \left\{-\pi\rho_\infty b^2 \frac{k^2U^2}{b^2} - 2\pi\rho_\infty b\left(\left[(\frac{-jkU}{2b}) + \alpha_1\beta_1\frac{U}{b}\cdot \left(-\frac{k(k+j\beta_1)}{k^2+\beta_1^2}\right) + \alpha_2\beta_2\frac{U}{b}\left(-\frac{k(k+j\beta_1)}{k^2+\beta_2^2}\right)\right]\right\}\bar{w}e^{i\omega t} \tag{17}$$

and in the nondimentional form as:

$$Lp(k) = \frac{L}{C_{L_\alpha}\frac{\dot{w}}{U}\rho_\infty U^2 b} \tag{18}$$

or

$$Lp(k) = \frac{-k - 2\left[-\frac{j}{2} + \alpha_1\beta_1\left(-\frac{k+j\beta_1}{k^2+\beta_1^2}\right) + \alpha_2\beta_2\left(-\frac{k+j\beta_2}{k^2+\beta_2^2}\right)\right]}{2j} \tag{19}$$

Under assumed conditions, the exact answer for the considered lift force is given by [1] and [5]:

$$L_{exact} = C1(k) = C(k) + \frac{jk}{2} \tag{20}$$

To compare our obtained result (i.e. Eq. (19)) with the exact solution (i.e. Eq.(20)), the real and imaginary parts of both equations are plotted versus k (see Figs. 2,3). As it is seen from these figures, very good agreements exist between our proposed relation and the exact one.

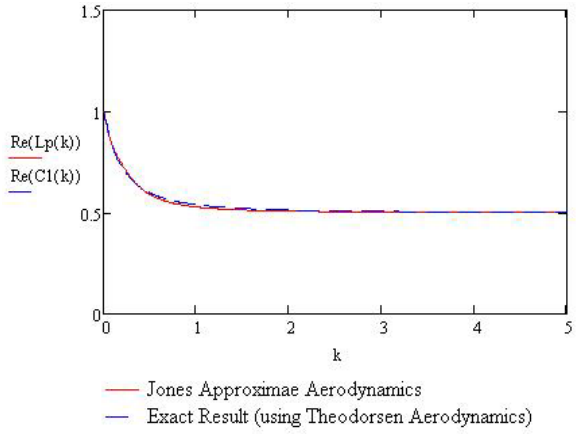

Fig. 2- plot of real part of non dimensional lift $Lp(k)$ versus k

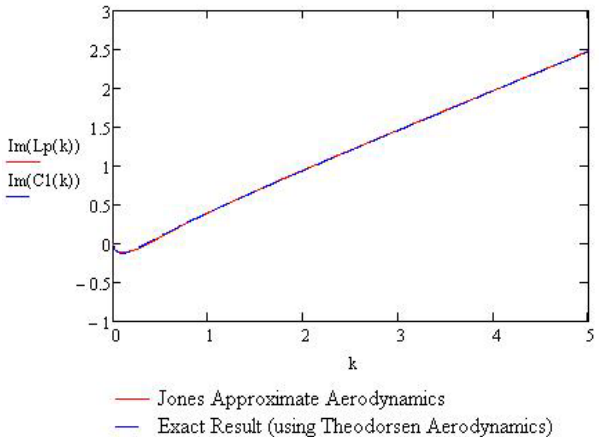

Fig. 3- plot of imaginary part of non dimensional lift $Lp(k)$ versus k

III. DYNAMICAL AEROELASTICITY FOR A 2-D TYPICAL SECTION MODEL

We recall the following expression for aerodynamic equations [1]:

$$[M_s]\{\ddot{q}\}+[C_s]\{\dot{q}\}+[K_s]\{q\}=\{F_{aerodynamic}\} \quad (21)$$

in which $\{F_{aerodynamic}\}$ includes the both lifting force and pitching moment given by Eq. (6) and Eq. (7), $[M_s]$, $[C_s]$ and $[K_s]$ are the structural mass matrix, the structural damping matrix and structural stiffness matrix respectively. After substituting expressions for aerodynamic loadings from Eq. (6) and Eq. (7), transferring the $\{q\}$ coordinate system into the generalized coordinate system $\{p\}$, and doing some further simplifications, one would get:

$$[M_s+M_a]\{\ddot{p}\}+[C_s+C_a]\{\dot{p}\}+[K_s+K_a]\{p\}=\{0\} \quad (22)$$

in which $[M_a]$, $[C_a]$ and $[K_a]$ are the aerodynamic mass matrix, the aerodynamic damping matrix and the aerodynamic stiffness matrix, respectively and $\lfloor p \rfloor = \lfloor h(\equiv w) \quad \theta \rfloor$

The structural matrix forms of above matrices are [1]:

$$[M_s]=\begin{pmatrix} m & S_\alpha \\ S_\alpha & I_\alpha \end{pmatrix}, C_s=\begin{pmatrix} c_h & 0 \\ 0 & c_\theta \end{pmatrix} \text{and } K_s=\begin{pmatrix} k_h & 0 \\ 0 & k_\theta \end{pmatrix} \quad (23)$$

where the modified aerodynamic matrices become[1] and [5]:

$$M_a=\begin{pmatrix} 1 & -b.a \\ -b.a & b^2(\frac{1}{8}+a^2) \end{pmatrix}\pi\rho_\infty b^2,$$

$$C_a=\frac{q.C.2\pi}{U}\begin{pmatrix} \frac{1}{2} & \frac{3b}{4}-\frac{b.a}{2} \\ -\frac{b}{2}(\frac{1}{2}+a) & \frac{b}{2}^2\ (a^2-a+\frac{1}{2}) \end{pmatrix}$$

and

$$K_a=\frac{q.C.2\pi}{U}\begin{pmatrix} -\frac{1}{b}k\left[\alpha_1\beta_1\left(-\frac{(k+j\beta_1)}{k^2+\beta_1^2}\right)+\alpha_2\beta_2\left(-\frac{(k+j\beta_2)}{k^2+\beta_2^2}\right)\right] & \frac{1}{2} \\ (\frac{1}{2}+a)k\left[\alpha_1\beta_1\left(-\frac{(k+j\beta_1)}{k^2+\beta_1^2}\right)+\alpha_2\beta_2\left(-\frac{(k+j\beta_2)}{k^2+\beta_2^2}\right)\right] & -\frac{b}{2}(\frac{1}{2}+a) \end{pmatrix} \quad (24)$$

in which $q=\frac{1}{2}\rho_\infty U^2$.

IV. DETERMINATION OF FLUTTER CHARACTERISTICS

Consider an airfoil with the following data:

$m=19.6(kg)$ *mass of airfoil*

$I=0.1236(kg.m^2)$ *Moment of inertia about C.G axis*

$k_h=1962(N.m)$ *Bending stiffness*

$k_\theta=2564(N.m/Rad)$ *Torsional stiffness*

$C=1.83(m)$ *Length of chord*

$a=-0.2$ *Distance coefficient* (*elastic axis to mid chord*)

$x_\theta=0.4$ *Distance coefficient* (*C.G. to mid chord*)

For a typical section with above mentioned specifications and parameters, a computer code using Eq. (22) is developed by which the flutter speed is determined using improved *p* and *p-k* methods. The outcomes of this program are illustrated on Figs. 4-7. Our calculations for flutter speed from both methods are as below

From improved *p* method results are:

$U_f=34.4\ (m/s)$, *Flutter speed*

$\omega_f=40.2\ (Rad/s)$, *Flutter frequency*

and from improved *p-k* method results are:

$U_f=35.5\ (m/s)$, *Flutter speed*

$\omega_f=43.6\ (Rad/s)$, *Flutter ferquency*

If we focus on result curves, for example according to Fig.4 which shows the variation of damping part of system's response versus free stream velocity, we can obtain flutter

speed of proposed airfoil when the damping becomes zero. Also it is possible to obtain the frequency of response for each free stream velocity, more specifically at the flutter speed (see Fig. 5). Similar trend has been followed to determine the flutter speed and flutter frequency using improved *p-k* method and the results are shown in Figs. 6-7

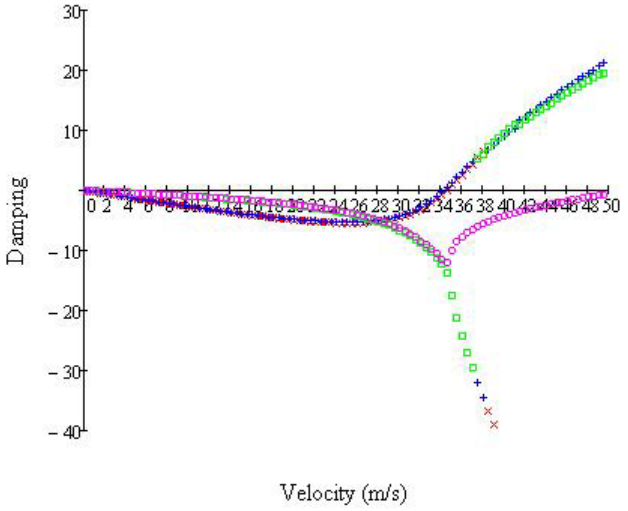

Fig. 4 Variation of damping vs. free stream velocity for airfoil, using improved *p* method

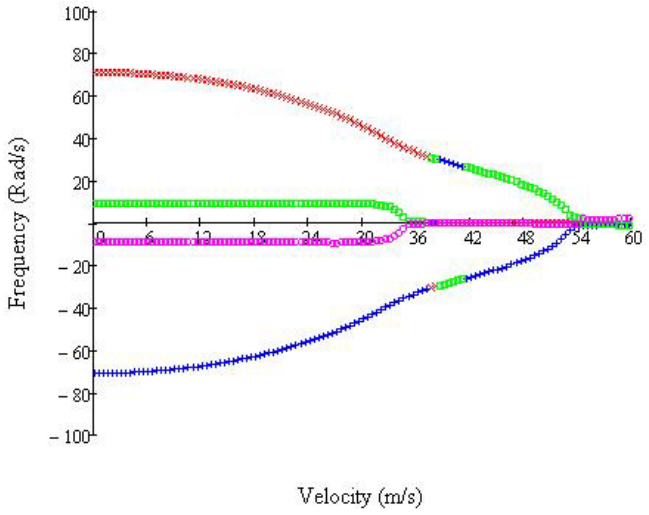

Fig. 5 Variation of frequency vs. free stream velocity for airfoil, using improved *p* method

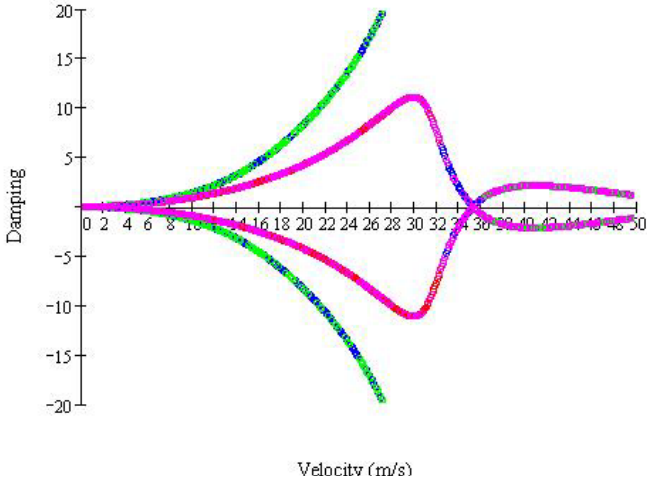

Fig. 6 Variation of damping vs. free stream velocity for airfoil, using improved *p-k* method

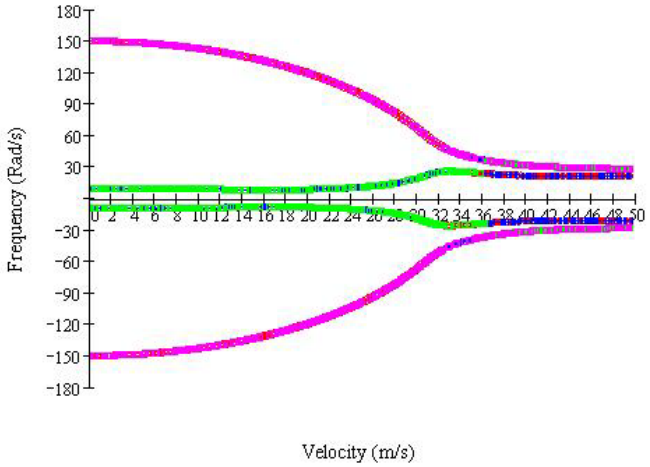

Fig. 7 Variation of frequency vs. free stream velocity for airfoil, using improved *p-k* method

V. GUST EFFECTS

Here we consider the sharp edged gust as an excitation function in the right hand side of the governing Eq. (22) of dynamic behavior of the system. Now, we obtain the system response due to the sharp edged gust in the time-domain solution. To solve the new governing differential equation for this case, we propose the following method by which the induced two coupled second order differential equations can be converted into four first order ordinary differential equations. This indeed will significantly facilitate the solution of the problem. Let's begin with the main differential equation as;

$$[M_s + M_a]\{\ddot{p}\} + [C_s + C_a]\{\dot{p}\} + [K_s + K_a]\{p\} = \{Q_{gust}\} \quad (25)$$

in which $\{Q_{gust}\}$ is a function of lift force, $L(t)$, and twisting moments, $M(t)$ as [1] and [5]:

$$L(t) = -2\pi\rho U_\infty b[g(s) - h(s)] \quad (26)$$

$$M_y(t) = -2\pi\rho U_\infty b^2(\frac{1}{2} + a)[g(s) - h(s)] \quad (27)$$

in which [1-4]

$$g(s) = w_{a3/4}(0).\Phi(s) + \int_0^s \frac{dw_G}{d\sigma}.\Phi(s-\sigma)d\sigma \quad (28)$$

$s = \frac{Ut}{b}$, $\sigma = \frac{Ut^*}{b}$ and [1-4]

$$\Phi(s) = 1 - 0.165e^{0.0455.s} - 0.33e^{0.3.s} \quad (29)$$

and [1-4]

$$h(s) = w_G(0).\Psi(s) + \int_0^s \frac{dw_G}{d\sigma}.\Psi(s-\sigma)d\sigma \quad (30)$$

where we estimate Kussner function $\Psi(s)$ expression in sharp edged gust problem in exponential form as Jones approximation [1-4]:

$$\Psi(s) = 1 - \frac{1}{2}e^{-0.13.s} - \frac{1}{2}e^{-s} \quad (31)$$

By introducing relations (26) and (27) into Eq. (25), decoupling and expanding resulted equations, one would get:

$$\begin{cases} a_1\ddot{h}(t) + a_2\dot{h}(t) + a_3h(t) + a_4\ddot{\theta}(t) + a_5\dot{\theta}(t) + a_6\theta(t) = F_1(t) \\ a_7\ddot{h}(t) + a_8\dot{h}(t) + a_9h(t) + a_{10}\ddot{\theta}(t) + a_{11}\dot{\theta}(t) + a_{12}\theta(t) = F_2(t) \end{cases} \quad (32)$$

where $F_1(t)$ and $F_2(t)$ are time domain excitation function,

By introducing some useful new auxiliary variables as:

$$\begin{cases} \ddot{h} = \dot{x}_2 \\ \dot{h} = x_2 \\ h = x_1 \\ \ddot{\theta} = \dot{x}_4 \\ \dot{\theta} = x_4 \\ \theta = x_3 \end{cases} \quad (33)$$

and

$$\begin{cases} \dot{x}_1 = x_2 \\ \dot{x}_3 = x_4 \end{cases} \quad (34)$$

we can express system of Eq.(32) as:

$$[M]\{\dot{\vec{x}}\} + [N]\{\vec{x}\} = [\Re]\{\vec{U}\} \quad (35)$$

where $\{\vec{x}\} = \{x_1 \ x_2 \ x_3 \ x_4\}^T$ is called vector space function. The expanded matrix form of Eq. (35) is:

$$[M] = \begin{bmatrix} 0 & a_1 & 0 & a_4 \\ 0 & a_7 & 0 & a_{10} \\ 1 & 0 & 0 & 0 \\ 0 & 0 & 1 & 0 \end{bmatrix}, \quad [N] = \begin{bmatrix} a_3 & a_2 & a_6 & a_5 \\ a_9 & a_8 & a_{12} & a_{11} \\ 0 & -1 & 0 & 0 \\ 0 & 0 & 0 & -1 \end{bmatrix}$$
$$[\Re] = \begin{bmatrix} 1 & 0 & 0 & 0 \\ 0 & 1 & 0 & 0 \\ 0 & 0 & 0 & 0 \\ 0 & 0 & 0 & 0 \end{bmatrix}, \quad \{U\} = \{F_1 \ \ F_2 \ \ 0 \ \ 0\}^T \quad (36)$$

Eq. (32) can be put into the following form as:

$$\{\dot{\vec{x}}\} = [A]\{\vec{x}\} + [B] \quad (37)$$

where

$$[A] = -[M]^{-1}[N] \quad (38)$$

and

$$[B] = [M]^{-1}[\Re]\{U\} \quad (39)$$

Note that the Eq. (37) is expressed in the state space form.

Now let us calculate the effect of sharp edged gust on this airfoil. In this step we compare the time response to a sharp edged gust with 2 (m/s) velocity for a typical section with data mentioned as before. The Eq. (37) is solved for three different speeds relative to the flutter speed as: $0.99U_f, U_f$ and $1.01U_f$.

Figs. 8-10 show the variation of vertical displacement of elastic center of the airfoil vs. time, under three different speeds relative to the flutter speed. As it is seen from these three figures, e.g. in the case where the gust speed is less than free air speed (Fig. 8), the vibration of airfoil will be damped out as we march through time. One of the reason for this kind of behavior might be the airfoil energy lose to the environment. Furthermore, in the case where the gust speed becomes equal to the free air stream velocity (Fig. 9), the vibration of airfoil will continue with constant alternating amplitude by time. It has been observed that by increasing the gust speed in this case the vibration amplitude becomes even greater, this can be interpreted that, the same energy transfer exists between airfoil and surrounding. Finally, when the speed of gust becomes greater than free stream velocity (Fig. 10), it means that surrounding air has higher energy level than airfoil motion and hence the amplitude of the vibration increases with a positive rate and it is in this case that a catastrophic fracture may occur.

The results for variation of pitching angel vs. time for the problem under consideration are plotted vs. time in Figs. 11-13, again for the three different speeds relative to the flutter speed as: $0.99U_f, U_f$ *and* $1.01U_f$. The same trend depicted in Figs. 8-10 are seen in these figures.

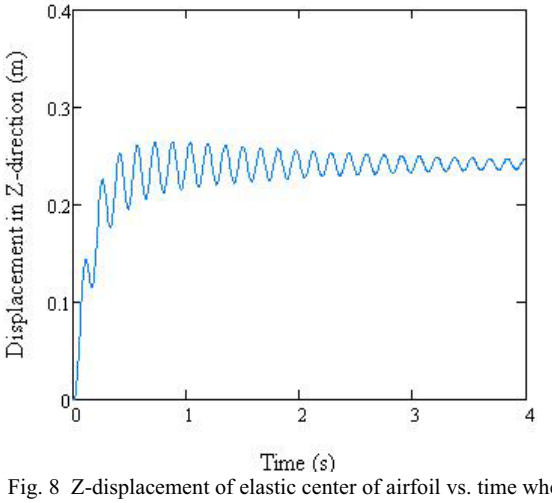

Fig. 8 Z-displacement of elastic center of airfoil vs. time when $U_\infty = 0.99U_f$

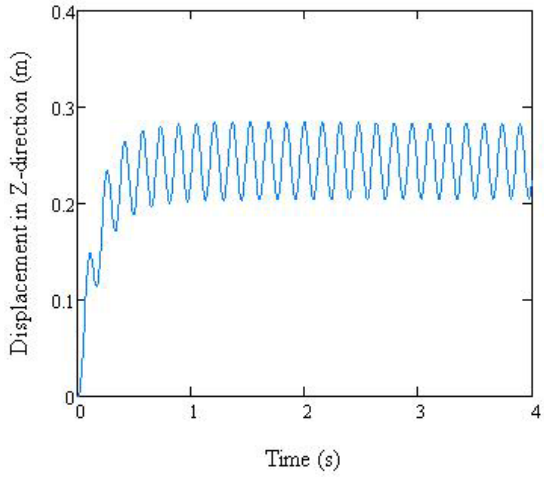

Fig. 9 Z-displacement of elastic center of airfoil vs. time when $U_\infty = U_f$

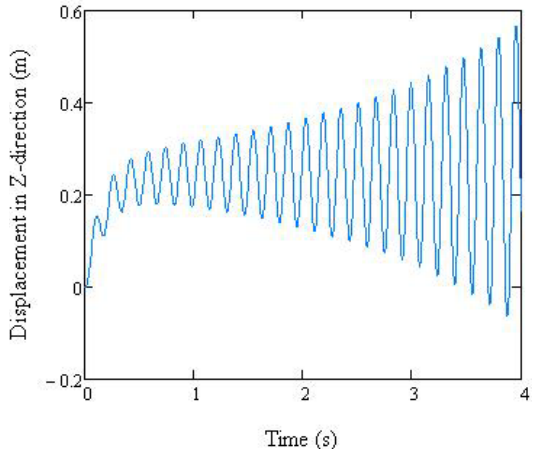

Fig. 10 Z-displacement of elastic center of airfoil vs. time when $U_\infty = 1.01U_f$

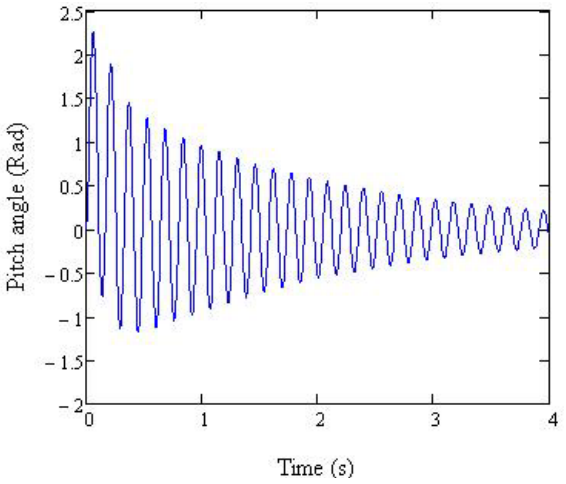

Fig. 11 Pitch angle of airfoil vs. time when $U_\infty = 0.99U_f$

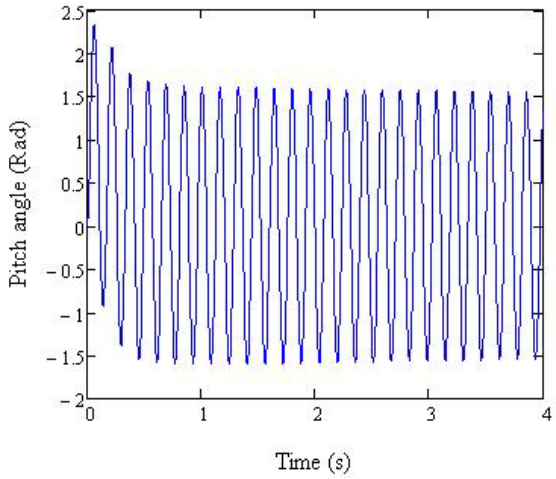

Fig. 12 Pitch angle of airfoil vs. time when $U_\infty = U_f$

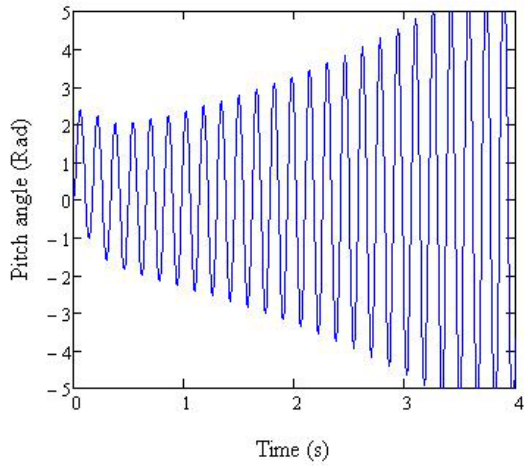

Fig. 13 Pitch angle of airfoil vs. time when $U_\infty = 1.01U_f$

VI. Conclusion

Based on the finite state Jones approximate aerodynamic model the obtained results of airoservoelastic behavior of considered airfoil subjected to three different speeds relative to the flutter speed, following conclusions are derived:

1- For the gust speed less than the free air speed the vibration of airfoil will be damped out as we march through time.

2- For the gust speed equal to the free air stream velocity, the vibration of airfoil will continue with constant alternating amplitude by time.

3- For the gust speed greater than free stream velocity the amplitude of the vibration increases by time with a positive rate and hence, a catastrophic fracture is predicted.

References

[1] D. H. Hodges, G. A. Pierce, "Introduction to Structural Dynamics and Aeroelasticity," New York: Cambridge University Press, 2002.

[2] E. H. Dowel, "A Modern Course in Aeroelasticity," 1995, Kluwer Academic Publishers.

[3] E. H. Dowel, "Aeroelasticity of Plates and Shells," Noordhoff International Publishing, 1975.

[4] R. L. Bisplinghoff, H. Ashley, R. L. Halfman "Aeroelasticity," Addisom-Wesley Publishing Co. Inc., 1955.

[5] D. A. Peters, W. M. Cao, "Finite state induced flow models, Part I: Two-dimensional thin airfoil," *Journal of Aircraft*, vol. 32, No. 2, March-April 1995, pp. 313-322.

[6] B. Ghadiri, M. Razi, "Limite cycle oscillations of rectatangular cantilever wings containing cubic nonlinearity in an incompressible flow," *Journal of solid and structures*, vol. 23, 2007, pp. 665-680.

[7] X.Chen, G. C. Zha, M. T. Yang, "Numerical simulation of 3-D wing flutter with fully coupled fluid-structural interaction," *Computers & Fluids*, vol. 36, 2007, pp. 856-867.

[8] M.R. Moosavi, A.R. Nadaf Oskouei, A. Khlil, "Flutter of subsonic wing," *Thin- Walled Structures*, vol. 43, 2005, pp. 617–627.

[9] S.A. Fazelzadeh, S. H. Pourtakdoust, N. Asadian, "Stochastic analysis of two dimensional nonlinear panels with structural damping uder random excitation," *Aerospace Science and Technology,* vol. 10, 2006, pp. 192–198.

[10] P. Svacek, M. Feistauer, J. Horacek, "Numerical simulation of flow induced airfoil vibrations with large amplitudes," *Journal of Fluids and Structures*, vol. 23, 2007, pp. 391–411.

[11] H. Haddadpour, R. D. Firouz-Abadi, "Evalution of quasi-steady aerodynamic modeling for flutter prediction of aircraft wings in incompressible flow," *Thin Walled Structures*, vol. 44, 2006, pp. 931–936.

[12] Z. Qin, P. Marzocca, L. Librescu, " Aeroelastic instability and response of advanced aircraft wings at subsonic flight speeds," *Aerospace Science and Technology*, vol. 6 , 2002, pp. 195–208.